

## EFFECT OF LIMITED OXYGEN GAS FLUX ON PROPERTIES OF Al-DOPED ZnO FILMS

Le Van Tri<sup>1\*</sup>, Tran Bao Quan<sup>1\*</sup>, Nguyen Khac Binh<sup>2</sup>, Vo Thi Ngoc Thuy<sup>3</sup>, Do Thi Hue<sup>4</sup>,  
Ngo Hai Dang<sup>1</sup>, and Pham Thi Kim Hang<sup>1\*</sup>

<sup>1</sup>Faculty of Applied Sciences, Ho Chi Minh City University of Technology and Education,  
Ho Chi Minh City, Vietnam

<sup>2</sup>VKTECH Research Center, Nguyen Tat Thanh University, Ho Chi Minh City, Vietnam

<sup>3</sup>University of Science, Vietnam National University Ho Chi Minh City, Vietnam

<sup>4</sup>TNU - University of Education, Thai Nguyen city, Vietnam

\*Corresponding author: Pham Thi Kim Hang, Email: hangptk@hcmute.edu.vn

### Article history

Received: 25/5/2024; Received in revised form: 06/6/2024; Accepted: 25/6/2024

### Abstract

*In this study, Al-doped ZnO thin films were sputter deposited on glass substrate as a function of limited oxygen gas inlet. The crystal structure, optical, and electrical properties of the films were characterized using X-ray diffraction, scanning electron microscopy, UV-Vis spectroscopy, and Hall measurement. High crystallinity was found in all AZO samples. Surface morphology presented small grain size of ~ 50 – 100 nm, and thickness of AZO thin films were maintained approximately at 280 nm. Average optical transmittance of AZO films was about 90% in the 450 – 600 nm region, and optical band-gap values varied from 3.327 to 3.380 eV. The electrical resistivity of AZO films decreased with an increasing amount of oxygen flux. These AZO films are quite appropriate for the perspective development of UV photodetectors as a central role absorbing components or n-type semiconducting layers.*

**Keywords:** AZO thin films, electrical properties, oxygen concentration, optical properties, RF-magnetron sputtering, UV-photodiode.

---

DOI: <https://doi.org/10.52714/dthu.13.5.2024.1295>

Cite: Le, V. T., Tran, B. Q., Nguyen, K. B., Vo, V. T., Do, T. H., Ngo, D. D., & Pham, T. K. H. (2024). Effect of limited oxygen gas flux on properties of Al-doped ZnO films. *Dong Thap University Journal of Science*, 13(5), 113-120. <https://doi.org/10.52714/dthu.13.5.2024.1295>.

Copyright © 2024 The author(s). This work is licensed under a CC BY-NC 4.0 License.

# ẢNH HƯỞNG CỦA LƯU LƯỢNG NHỎ DÒNG KHÍ OXY ĐỐI VỚI CÁC TÍNH CHẤT CỦA MÀNG ZnO PHA TẠP Al

Lê Văn Trí<sup>1\*</sup>, Trần Bảo Quân<sup>1\*</sup>, Nguyễn Khắc Bình<sup>2</sup>, Võ Thị Ngọc Thủy<sup>3</sup>, Đỗ Thị Huệ<sup>4</sup>,  
Ngô Hải Đăng<sup>1</sup> và Phạm Thị Kim Hằng<sup>1\*</sup>

<sup>1</sup>Khoa Khoa học ứng dụng, Trường Đại học Sư phạm Kỹ thuật Thành phố Hồ Chí Minh,  
Thành phố Hồ Chí Minh, Việt Nam

<sup>2</sup>Trung tâm VKTech - Viện kỹ thuật Công nghệ cao, Trường Đại học Nguyễn Tất Thành,  
Thành phố Hồ Chí Minh, Việt Nam

<sup>3</sup>Trường Đại học Khoa học Tự nhiên, Đại học Quốc gia Thành phố Hồ Chí Minh, Việt Nam

<sup>4</sup>Trường Đại học Sư phạm, Đại học Thái Nguyên, thành phố Thái Nguyên, Việt Nam

\*Tác giả liên hệ: Phạm Thị Kim Hằng, Email: hangptk@hcmute.edu.vn

## Lịch sử bài báo

Ngày nhận: 25/5/2024; Ngày nhận chỉnh sửa: 06/6/2024; Ngày chấp nhận: 25/6/2024

## Tóm tắt

Trong nghiên cứu này, màng mỏng ZnO pha tạp Al được mọc để thủy tinh với một lượng nhỏ khí oxy. Cấu trúc tinh thể, tính chất quang và tính chất điện của màng được phân tích bằng nhiễu xạ tia X, kính hiển vi điện tử quét, quang phổ UV-Vis và phép đo Hall. Độ kết tinh cao được tìm thấy trong tất cả màng AZO. Hình thái bề mặt có kích thước hạt nhỏ khoảng 50 – 100 nm và độ dày của màng mỏng AZO xấp xỉ 280 nm. Độ truyền qua trung bình của màng AZO khoảng 90% trong vùng bước sóng 450 – 600 nm và các giá trị độ rộng vùng cấm quang được xác định từ 3.327 đến 3.380 eV. Điện trở suất của màng AZO giảm khi tăng lưu lượng khí oxy. Kết quả nghiên cứu này thích hợp để ứng dụng vào bộ tách sóng quang UV, trong đó màng AZO đóng vai trò trung tâm và hấp thụ các thành phần hoặc lớp bán dẫn loại n.

**Từ khóa:** Đi-ốt quang UV, lưu lượng khí oxy, màng mỏng AZO, phun xạ RF-magnetron, tính chất điện, tính chất quang.

## 1. Introduction

In recent decades, knowledge and usage of transparent conductive oxide (TCO) films in photonic and optoelectronic devices have made extensive progress (Ma & He, 2011; Yun & Kim, 2012). Among TCO family, indium tin oxide (ITO) film with great transparency in the visible range and good electrical conductivity, has been widely used in OLED (H. Kim et al., 1999), solar cells (Lien, 2010),... However, high cost of indium component has put limits on its broad application (Chavan et al., 2023). Therefore, different potential substitutes have emerged such as doped  $\text{SnO}_2$ ,  $\text{TiO}_2$ ,... Recently, ZnO film has turned out to be a favorable candidate for its low cost, environmental friendliness, very good transparency in the visible range and good electrical conductivity. Moreover, ZnO films represent high crystallinity, good thermal conductivity, and good ability to deposit on plastic and glass substrates even at low temperatures.

In addition, ZnO is a wide bandgap semiconductor ( $E_g \sim 3.37$  eV) and has a large exciton binding energy ( $\sim 60$  meV) at room temperature (Borysiewicz, 2019). ZnO exhibits inherently n-type semiconducting properties due to intrinsic defects such as oxygen vacancies ( $V_o$ ) and zinc interstitials ( $Zn_i$ ). The ZnO carrier concentration and mobility are typically found in the range of  $10^{16} - 10^{17}$  và  $20 - 400$   $\text{cm}^2\text{V}^{-1}\text{s}^{-1}$ , respectively (Vyas, 2020).

The optical properties of ZnO have also been extensively studied, with some reports indicating that the transmittance of ZnO films can reach over 80% in visible light (Lai & Lee, 2008; Mekhnache et al., 2011). However, for TCO materials, the simultaneous existence of high conductivity and transparency is always a major challenge that receives much research interest. Several works pointed out that by doping group III elements (B (Wenas et al., 1991), Ga (Bhosle et al., 2006), Al (Maldonado & Stashans, 2010), In (Kumar et al., 2004)) into ZnO films, electrical resistivity could be reduced and optical transparency in the visible range could be increased. Especially, Al-doped ZnO (AZO) is widely studied for its low cost, non-toxicity, and high thermal stability. Moreover, the electrical and optical properties of Al-doped ZnO films have been investigated in different reports, paving the way for tremendous application of AZO films in solar cells (Badgujar et al., 2022), OLEDs (Choi et al., 2013),... However, the optical and electrical properties of

AZO films are quite sensitive to deposition and post-deposition conditions. Different methods have been employed to prepare high-quality AZO films such as metal-organic chemical vapor deposition (MOCVD) (Fragala et al., 2009), sputtering (Fang et al., 2002), atomic layer deposition (ALD) (Choi et al., 2013), sol-gel (Lee et al., 2009). Among them, RF-magnetron sputtering is the most popular technique for AZO because of its ability to deposit on large areas with high deposition rate, good adhesion between the film and the substrate, low processing temperature, and ease in adjusting parameters during deposition (Fang et al., 2002; Park et al., 2006).

In this report, AZO thin films were prepared on glass substrates with RF-magnetron sputtering by introducing small oxygen gas flows (0.2 - 0.8 sccm). Crystal structures of AZO thin films were studied using X-ray diffraction (XRD) in range of  $20 - 80^\circ$ . The surface morphology and thickness of AZO films were observed using scanning electron microscopy (SEM). The optical properties of AZO films were analyzed using UV-Vis spectroscopy in the range of visible to near-infrared regions. The electrical properties of AZO films were characterized with Hall-effect measurement.

## 2. Experiments

AZO thin films were prepared by radio frequency (RF)-magnetron sputtering on glass substrates using 2% Al-doped ZnO lab-made targets. They were subjected to one-day planet milling, disk shaping, and three-hour sintering at  $1400^\circ\text{C}$ . The total sintering process (ramping, sintering, and cooling) took approximately 30 hours. The glass substrates were cleaned by acetone, ethanol, and isopropyl alcohol (IPA) for 5 min each, respectively. To eliminate contaminants and moisture still present on the glass substrate surface, the substrates were heated in a vacuum chamber remained at  $5 \times 10^{-3}$  Torr. The growth temperature of AZO films was maintained at  $200^\circ\text{C}$  and power of 50W. The argon gas flow was fixed at 60 sccm while the oxygen gas flow was set at 0.2 sccm (sample 1), 0.4 sccm (sample 2), 0.6 sccm (sample 3), and 0.8 sccm (sample 4). The crystal structure of the AZO films was analyzed using X-ray diffraction (XRD). Scanning electron microscopy (SEM) and UV-VIS spectroscopic analysis were employed to study the surface morphology and transmittance properties. Hall measurement was used to characterize the electrical property.

### 3. Results and discussion

Figure 1a shows XRD pattern of the AZO thin film deposited with various oxygen gas flow rates. The sharp and well-defined peaks of (002) are observed in all AZO samples. The (002) plane of AZO films corresponds to a diffraction angle value of  $2\theta \sim 34^\circ$ , showing the hexagonal structure of wurtzite and the high intensity growth orientation along the c-axis direction as the oxygen content progressively rises (Hwang et al., 2011; Otieno et al., 2019) (see Fig. 1b). The absence of diffraction peaks for aluminum and its compound indicates that aluminum atoms may have replaced Zn in the lattice location or locate at interstitial sites (Fragala et al., 2009). Moreover, a small increase in oxygen inlet leads to highly improved crystallinity, resulting in

larger grain sizes and a reduction of full width at half maximum (FWHM) (see Fig.1c) (Cao et al., 2014). When increasing the oxygen gas rate, the d-spacing value tends to decrease as well. This could be due to the different stress and strain emerging during the AZO film deposition process, which lowers the values of the lattice constant (see Fig.1d) (Bose et al., 2018). The films are in compressive stress conditions along the c-axis since the obtained stress along the c-axis presents negative values. The former component can be ascribed to a thermal mismatch between AZO films, and substrate and generation mechanism of the latter can be accredited to the growth process itself (Li et al., 2008). Evidently, small change in oxygen gas inlet produced greatly effects on the structure properties of AZO films.

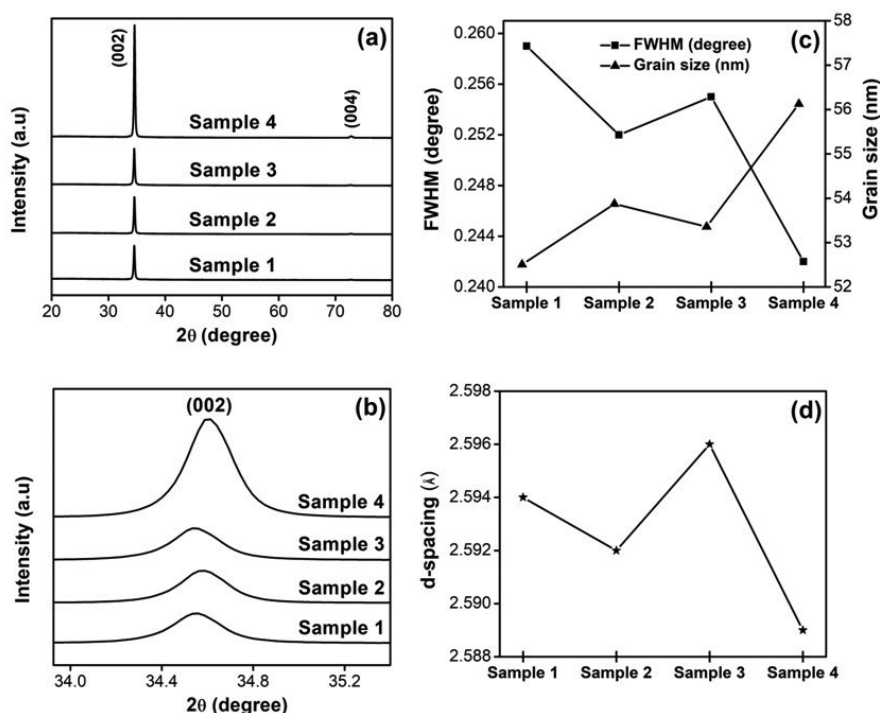


Figure 1. (a) XRD spectra, (b) XRD peak in the narrow range, (c) Full width at half maximum (FWHM) of XRD (002) peaks and grain sizes, and (d) d-spacing of AZO samples as the function of small oxygen inlet

Table 1. Information about structural properties obtained from the XRD spectra

Sample	$2\theta$ ( $^\circ$ )	FWHM ( $^\circ$ )	Grain size (nm)	c (Å)	d-spacing (Å)	Micro strain ( $\times 10^{-3}$ )
1	34.562	0.259	52.506	5.188	2.594	-3.341
2	34.588	0.252	53.874	5.184	2.592	-4.073
3	34.535	0.255	53.358	5.191	2.596	-2.605
4	34.614	0.242	56.125	5.180	2.589	-4.804

Figure 2 presents the SEM images of the surface morphology of the AZO thin films. The particle sizes of AZO were found in 50 – 100 nm. As the oxygen content increased, the surface AZO thin films became

smoother due to the etching effect (M. Kim et al., 2016). The cross-sectional SEM image shows the thickness of AZO thin films is about ~ 280 nm (see Fig 2e).

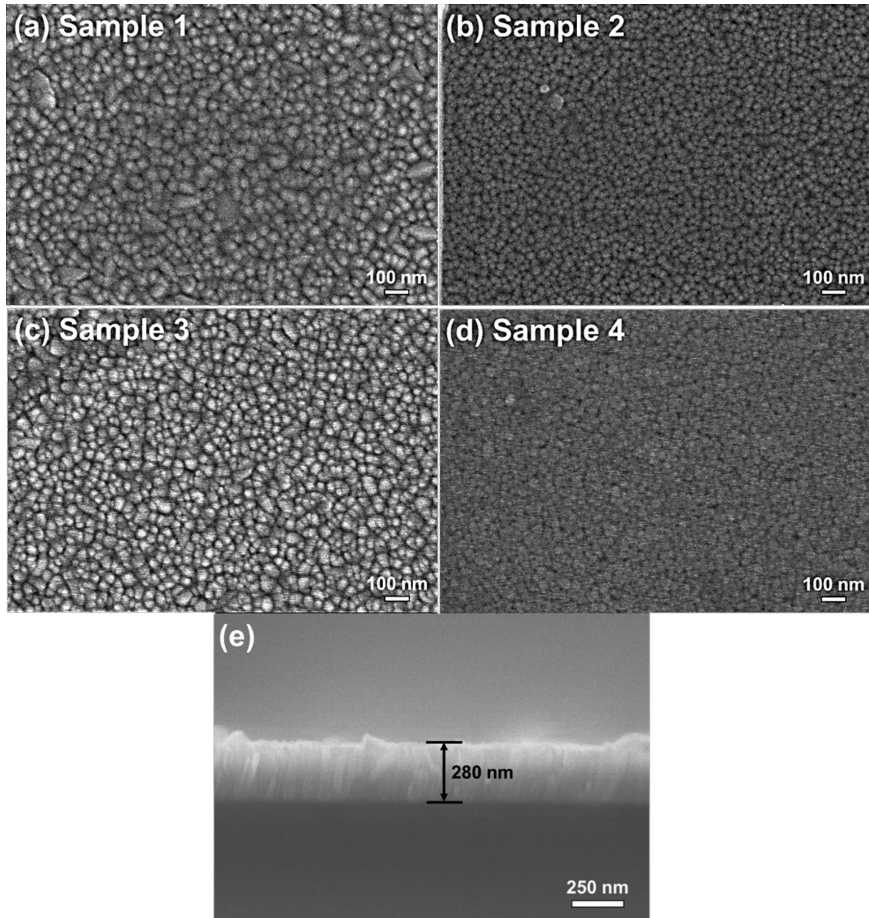


Figure 2. The top view of SEM images of (a) sample 1, (b) sample 2, (c) sample 3, and (d) sample 4, (e) the cross-sectional view of sample 3

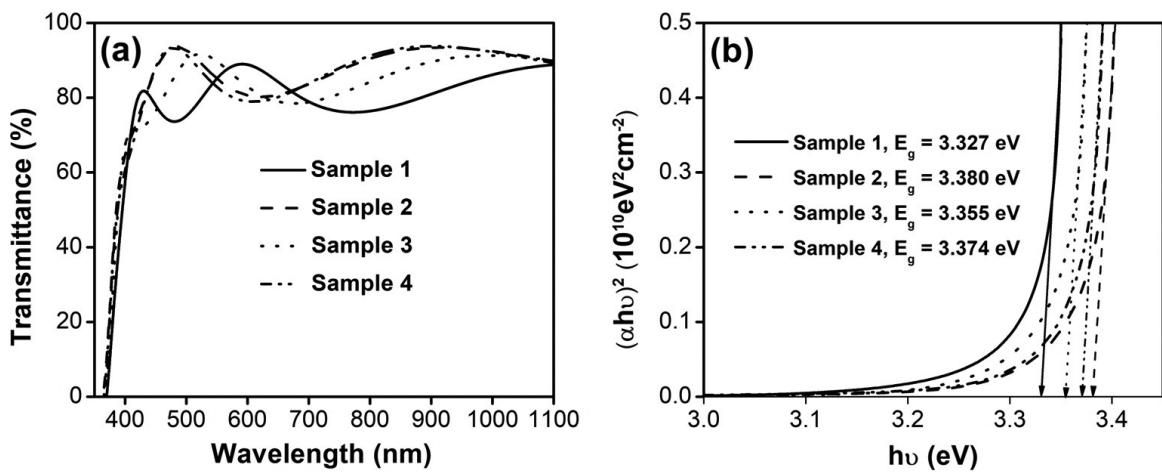


Figure 3. (a) Transmission spectra and (b) Tauc's plots used to estimate the optical band gap of AZO thin films as the function of small amount of oxygen flux

In Figure 3(a), all AZO films exhibit high average transmittance of more than 70% in the visible light spectrum, approaching to 90% in the 450 – 600 nm visible light area, and decreases significantly in the infrared spectrum. The transmittance of the AZO films was found to rise in the visible region as the oxygen flow increased. However, transmittance of sample 3 dropped as a result of re-sputtering occurring during the deposition process (Suchea et al., 2007). It goes in line with the SEM analysis since the incident light scattering will be reduced due to the relatively smooth surface as the oxygen content increases. Sample 1 exhibits the lowest transmittance; this could be attributed to the high density of point defects such as oxygen or Zn interstitial (Muchuweni et al., 2017).

The band gap energy ( $E_g$ ) of sputtered AZO thin film was obtained by applying well-known Tauc model and derivative spectroscopy techniques (Pankove, 1971). Fig. 3(b) shows the value of optical band gap fluctuated between 3.327 and 3.380 eV, which is consistent with the literature of ZnO (3.37 eV) (Özgür et al., 2005). The band gap slightly increases when the oxygen gas rates increase due to the shift of the absorption edge to shorter wavelengths

(see figure 3a), which could be explained by Burstein - Moss effect (Cao et al., 2014).

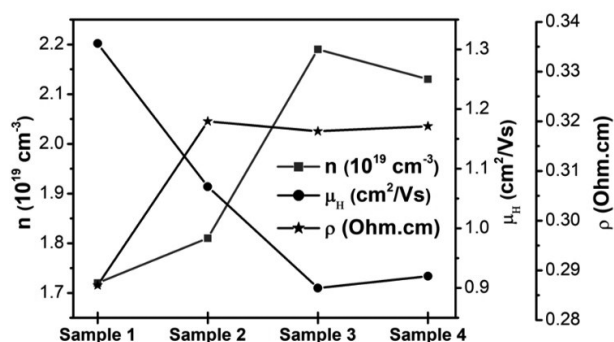


Figure 4. Carrier concentration (n), Hall mobility ( $\mu_H$ ) resistivity ( $\rho$ ) versus concentration Oxygen in the AZO thin films

Figure 4 presents the carrier concentration, mobility, and electrical resistivity of AZO thin films with a small oxygen inlet, as measured by the Hall technique. The following equation represents the relation between the resistivity ( $\rho$ ), carrier concentration (n), carrier charge (e), and mobility ( $\mu_H$ ):

$$\rho = \frac{1}{ne\mu} \quad (1)$$

Table 2. Optical and electrical properties of AZO thin films deposited as the function of small amount of oxygen flux

Sample	Optical properties		Electrical properties		
	Transmittance (400 - 800 nm)	Band gap (eV)	n ( $\times 10^{19}$ cm <sup>-3</sup> )	$\mu_H$ (cm <sup>2</sup> /Vs)	$\rho$ (Ohm.cm)
1	89%	3.327	1.72	1.31	0.278
2	94%	3.380	1.81	1.07	0.320
3	92%	3.335	2.19	0.90	0.318
4	93%	3.374	2.13	0.92	0.319

The resistivity of n-type AZO thin films increases with increasing in oxygen flux, which is in good agreement with the previous work (M. Kim et al., 2016). Carrier concentration values are  $1.72 \times 10^{19}$  cm<sup>-3</sup>,  $1.87 \times 10^{19}$  cm<sup>-3</sup>,  $2.19 \times 10^{19}$  cm<sup>-3</sup>, and  $2.13 \times 10^{19}$  cm<sup>-3</sup> for samples 1, 2, 3 and 4, respectively. These results show that the carrier concentration is enhanced by increasing the small amount of oxygen flux. It appears that the presence of additional oxygen during the deposition process could result in enhanced crystallinity, better replacement of aluminum ions at lattice sites. These all combine to an increase in carrier concentration. Mobility reduces as oxygen flux increases (see Table 2). Higher ionized impurity scattering and higher carrier concentration could

relate to the decreased tendency of carrier mobility (Badgujar et al., 2022; Hounq et al., 2007).

#### 4. Conclusion

In summary, aluminum-doped ZnO was deposited on glass substrate using RF-magnetron sputtering as a function of a small oxygen flux (0.2 - 0.8 sccm). The XRD analysis revealed a high quality of AZO crystalline and c-axis preferred orientation as the small oxygen inlet was introduced during the deposition process. Higher oxygen inlets result in smoother film surface morphology. The thickness is ~ 280 nm. Average optical transmittance is above 80% in the visible region. Bandgap values vary from 3.327 to 3.380 as oxygen flux increases. The

Hall measurement results present the low electrical resistivities ( $\sim 0.3 \text{ Ohm.cm}$ ), and high carrier concentration ( $\sim 10^{19} \text{ cm}^{-3}$ ). The obtained AZO films exhibit themselves as potential candidates for different photonic and optoelectronic applications such as UV-photodetectors, UV-LED, TFT and flat panel displays.

**Acknowledgments:** This work belongs to the project grant No: SV2024 - 46 funded by Ho Chi Minh City University of Technology and Education, Vietnam.

✧ *These authors contributed equally to this work.*

## References

- Badgujar, A. C., Yadav, B. S., Jha, G. K., & Dhage, S. R. (2022). Room Temperature Sputtered Aluminum-Doped ZnO Thin Film Transparent Electrode for Application in Solar Cells and for Low-Band-Gap Optoelectronic Devices. *ACS Omega*, 7(16), 14203–14210. <https://doi.org/10.1021/acsomega.2c00830>.
- Bhosle, V., Tiwari, A., & Narayan, J. (2006). Electrical properties of transparent and conducting Ga doped ZnO. *Journal of Applied Physics*, 100(3). <https://doi.org/10.1063/1.2218466>.
- Borysiewicz, M. A. (2019). ZnO as a functional material, a review. *Crystals*, 9(10). <https://doi.org/10.3390/cryst9100505>
- Bose, S., Arokiyadoss, R., Bhargav, P. B., Ahmad, G., Mandal, S., Barua, A. K., & Mukhopadhyay, S. (2018). Modification of surface morphology of sputtered AZO films with the variation of the oxygen. *Materials Science in Semiconductor Processing*, 79, 135–143. <https://doi.org/10.1016/j.mssp.2018.01.027>.
- Cao, P. J., Han, S., Liu, W. J., Jia, F., Zeng, Y. X., Zhu, D. L., & Lu, Y. M. (2014). Effect of oxygen flowrate on optical and electrical properties in Al doped ZnO thin films. *Materials Technology*, 29(6), 336–340. <https://doi.org/10.1179/175355714Y.0000000172>.
- Chavan, G. T., Kim, Y., Khokhar, M. Q., Hussain, S. Q., Cho, E. C., Yi, J., Ahmad, Z., Rosaiah, P., & Jeon, C. W. (2023). A Brief Review of Transparent Conducting Oxides (TCO): The Influence of Different Deposition Techniques on the Efficiency of Solar Cells. In *Nanomaterials*, 13(7). MDPI. <https://doi.org/10.3390/nano13071226>.
- Choi, Y. -J., Gong, S. C., Park, C. -S., Lee, H. -S., Jang, J. G., Chang, H. J., Yeom, G. Y., & Park, H.-H. (2013). Improved performance of organic light-emitting diodes fabricated on Al-doped ZnO anodes incorporating a homogeneous Al-doped ZnO buffer layer grown by atomic layer deposition. *ACS Applied Materials & Interfaces*, 5(9), 3650–3655. <https://doi.org/10.1021/am400140c>.
- Fang, G., Li, D., & Yao, B. -L. (2002). Fabrication and vacuum annealing of transparent conductive AZO thin films prepared by DC magnetron sputtering. *Vacuum*, 68(4), 363–372. [https://doi.org/10.1016/S0042-207X\(02\)00544-4](https://doi.org/10.1016/S0042-207X(02)00544-4).
- Fragala, M. E., Malandrino, G., Giangregorio, M. M., Losurdo, M., Bruno, G., Lettieri, S., Amato, L. S., & Maddalena, P. (2009). Structural, optical, and electrical characterization of ZnO and Al-doped ZnO thin films deposited by MOCVD. *Chemical Vapor Deposition*, 15(10-12), 327–333. <https://doi.org/10.1002/cvde.200906790>
- Houng, B., Huang, C. -L., & Tsai, S. -Y. (2007). Effect of the pH on the growth and properties of sol-gel derived boron-doped ZnO transparent conducting thin film. *Journal of Crystal Growth*, 307(2), 328–333. <https://doi.org/10.1016/j.jcrysgro.2007.07.001>.
- Hwang, D. -H., Ahn, J. -H., Hui, K. -N., Hui, K. -S., & Son, Y. -G. (2011). Effect of oxygen partial pressure contents on the properties of Al-doped ZnO thin films prepared by radio frequency sputtering. *Journal of Ceramic Processing Research*, 12(2), 150-154.
- Kim, H., Pique, A., Horwitz, J. S., Mattoussi, H., Murata, H., Kafafi, Z. H., & Chrisey, D. B. (1999). Indium tin oxide thin films for organic light-emitting devices. *Applied Physics Letters*, 74(23), 3444–3446. <https://doi.org/10.1063/1.124122>.
- Kim, M., Jang, Y. -J., Jung, H. -S., Song, W., Kang, H., Kim, E. K., Kim, D., Yi, J., & Lee, J. (2016). Influence of oxygen gas ratio on the properties of aluminum-doped zinc oxide films prepared by radio frequency magnetron sputtering. *Journal of Nanoscience and Nanotechnology*, 16(5), 5138–5142. <https://doi.org/10.1166/jnn.2016.12227>.

- Kumar, P. M. R., Kartha, C. S., Vijayakumar, K. P., Abe, T., Kashiwaba, Y., Singh, F., & Avasthi, D. K. (2004). On the properties of indium doped ZnO thin films. *Semiconductor Science and Technology*, 20(2), 120. <https://doi.org/10.1088/0268-1242/20/2/003>.
- Lai, L. -W., & Lee, C. -T. (2008). Investigation of optical and electrical properties of ZnO thin films. *Materials Chemistry and Physics*, 110(2–3), 393–396. <https://doi.org/10.1016/j.matchemphys.2008.02.029>.
- Lee, K. E., Wang, M., Kim, E. J., & Hahn, S. H. (2009). Structural, electrical and optical properties of sol–gel AZO thin films. *Current Applied Physics*, 9(3), 683–687. <https://doi.org/10.1016/j.cap.2008.06.006>.
- Li, L., Fang, L., Chen, X. M., Liu, J., Yang, F. F., Li, Q. J., Liu, G. B., & Feng, S. J. (2008). Influence of oxygen argon ratio on the structural, electrical, optical and thermoelectrical properties of Al-doped ZnO thin films. *Physica E: Low-Dimensional Systems and Nanostructures*, 41(1), 169–174. <https://doi.org/10.1016/j.physe.2008.07.001>.
- Lien, S. -Y. (2010). Characterization and optimization of ITO thin films for application in heterojunction silicon solar cells. *Thin Solid Films*, 518(21), S10–S13. <https://doi.org/10.1016/j.tsf.2010.03.023>.
- Ma, Z. Q., & He, B. (2011). TCO-Si based heterojunction photovoltaic devices. *Solar Cells-Thin-Film Technologies, InTech*, 111-137. <https://doi.org/10.1063/1.124122>.
- Maldonado, F., & Stashans, A. (2010). Al-doped ZnO: Electronic, electrical and structural properties. *Journal of Physics and Chemistry of Solids*, 71(5), 784–787. <https://doi.org/10.1016/j.jpcs.2010.02.001>.
- Mekhnache, M., Drici, A., Hamideche, L. S., Benzarouk, H., Amara, A., Cattin, L., Bernede, J. C., & Guerioune, M. (2011). Properties of ZnO thin films deposited on (glass, ITO and ZnO: Al) substrates. *Superlattices and Microstructures*, 49(5), 510–518. <https://doi.org/10.1016/j.spmi.2011.02.002>.
- Muchuweni, E., Sathiaraj, T. S., & Nyakoty, H. (2017). Effect of O<sub>2</sub>/Ar flow ratio on Ga and Al co-doped ZnO thin films by rf sputtering for optoelectronic device fabrication. *Materials Research Bulletin*, 95, 123–128. <https://doi.org/10.1016/j.materresbull.2017.07.029>.
- Otieno, F., Airo, M., Ganetsos, T., Erasmus, R. M., Billing, D. G., Quandt, A., & Wamwangi, D. (2019). Role of oxygen concentrations on structural and optical properties of RF magnetron sputtered ZnO thin films. *Optical and Quantum Electronics*, 51, 1–13. <https://doi.org/10.1007/s11082-019-2076-5>.
- Özgür, Ü., Alivov, Y. I., Liu, C., Teke, A., Reshchikov, M. A., Doğan, S., Avrutin, V., Cho, S. -J., & Morkoç, H. (2005). A comprehensive review of ZnO materials and devices. *Journal of Applied Physics*, 98(4). <https://doi.org/10.1063/1.1992666>.
- Pankove, J. I. (1971). Optical processes in semiconductors Prentice-Hall. *New Jersey*, 92, 36.
- Park, J. H., Shin, J. M., Cha, S. -Y., Park, J. W., Jeong, S. -Y., Pak, H. K., & Cho, C. -R. (2006). Deposition-temperature effects on AZO thin films prepared by RF magnetron sputtering and their physical properties. *Journal of the Korean Physical Society*, 49(9), 584.
- Sucnea, M., Christoulakis, S., Katsarakis, N., Kitsopoulos, T., & Kiriakidis, G. (2007). Comparative study of zinc oxide and aluminum doped zinc oxide transparent thin films grown by direct current magnetron sputtering. *Thin Solid Films*, 515(16), 6562–6566. <https://doi.org/10.1016/j.tsf.2006.11.151>.
- Vyas, S. (2020). A short review on properties and applications of zinc oxide based thin films and devices: ZnO as a promising material for applications in electronics, optoelectronics, biomedical and sensors. *Johnson Matthey Technology Review*, 64(2), 202–218. <https://doi.org/10.1595/205651320X15694993568524>.
- Wenas, W. W., Yamada, A., Takahashi, K., Yoshino, M., & Konagai, M. (1991). Electrical and optical properties of boron-doped ZnO thin films for solar cells grown by metalorganic chemical vapor deposition. *Journal of Applied Physics*, 70(11), 7119–7123. <https://doi.org/10.1063/1.349794>.
- Yun, J.-H., & Kim, J. (2012). Double transparent conducting oxide films for photoelectric devices. *Materials Letters*, 70, 4–6. <https://doi.org/10.1016/j.matlet.2011.11.053>.